bjh research paper

Actin filaments and microtubule dual-granule transport in human adhered platelets: the role of α-dystrobrevins

Doris Cerecedo,[1] Bulmaro Cisneros,[2] Ricardo Mondragón,[3] Sirenia González[4] and Iván J. Galván[5]

[1]Laboratorio de Hematobiología, Escuela Nacional de Medicina y Homeopatía, Instituto Politécnico Nacional (IPN), México DF, [2]Departamento de Genética y Biología Molecular, [3]Departamento de Bioquímica, [4]Unidad de Microscopía Electrónica, and [5]Unidad de Microscopía Confocal, Centro de Investigación y de Estudios Avanzados (CINVESTAV) del IPN, México DF, México

Received 5 November 2009; accepted for publication 17 November 2009

Correspondence: Dr Doris A. Cerecedo Mercado, Laboratorio de Hematobiología, Escuela Nacional de Medicina y Homeopatía, IPN, Guillermo Massieu Helguera no. 239, Col. La Escalera Ticomán, 07320 México, DF, México. E-mail: dcereced@prodigy.net.mx

Summary

Upon activation with physiological stimuli, human platelets undergo morphological changes, centralizing their organelles and secreting effector molecules at the site of vascular injury. Previous studies have indicated that the actin filaments and microtubules of suspension-activated platelets play a critical role in granule movement and exocytosis; however, the participation of these cytoskeleton elements in adhered platelets remains unexplored. α- and β-dystrobrevin members of the dystrophin-associated protein complex in muscle and non-muscle cells have been described as motor protein receptors that might participate in the transport of cellular components in neurons. Recently, we characterized the expression of dystrobrevins in platelets; however, their functional diversity within this cellular model had not been elucidated. The present study examined the contribution of actin filaments and microtubules in granule trafficking during the platelet adhesion process using cytoskeleton-disrupting drugs, quantification of soluble P-selectin, fluorescence resonance transfer energy analysis and immunoprecipitation assays. Likewise, we assessed the interaction of α-dystrobrevins with the ubiquitous kinesin heavy chain. Our results strongly suggest that microtubules and actin filaments participate in the transport of alpha and dense granules in the platelet adhesion process, during which α-dystrobrevins play the role of regulatory and adaptor proteins that govern trafficking events.

Keywords: granule dispersion, actin-based structures, granulomere, cytoskeleton remodelling, platelet adhesion.

The critical role of the platelet is to sense vascular damage and respond by secreting components that promote primary haemostasis and clot formation. Activated platelets initiate signalling cascades that lead to cytoskeletal re-organization, centralization of secretory granules, and exocytosis of small molecules and proteins from three classes of granules: dense core and α-granules and secretory lysosomes (Rendu & Brohard-Bohn, 2001). Platelet granules are the most prominent structural features, and upon activation, they coalesce in the centre of the platelet and fuse with the open canalicular system (OCS). The OCS represents a membrane reservoir that is evaginated onto the platelet surface during interaction with surfaces (Stenberg *et al*, 1984; Escolar *et al*, 1989), fusing with the plasma membrane (Ginsberg *et al*, 1980). The release of the granule contents into the OCS and their diffusion into the extracellular environment exert a paracrine role to activate other platelets in the immediate area that are critical to the formation of the haemostatic thrombus (Escolar & White, 1991; White & Escolar, 1991).

Dense core granules mainly contain small molecules, such as adenosine diphosphate (ADP), serotonin and calcium, which are critical for further platelet activation and vasoconstriction. α-Granules represent the storage sites for a diverse set of proteins, such as platelet factor 4, von Willebrand factor, platelet-derived growth factor and P-selectin, which play roles in clot formation and initiating wound healing. Platelets also release lysosomal enzymes, such as cathepsins and hexosaminidase, which may play a role in clot remodelling or in further platelet activation (Anitua *et al*, 2004). To date, more than 300 proteins and small molecules have been

First published online 8 February 2010
doi:10.1111/j.1365-2141.2010.08085.x

© 2010 Blackwell Publishing Ltd,

shown to be secreted from activated platelets (Coppinger *et al*, 2004).

Studies performed in suspended platelets have shown contradictory arguments for the participation of microtubules or microfilaments. One study demonstrated that microtubules are intimately involved in the movement of intracellular granules (Sneddon, 1971); other studies that induced the stabilization of microtubules with taxol did not inhibit the secretion process (White & Rao, 1982, 1983). It has also been demonstrated that actin polymerization, granule centralization and membrane fusion act synergistically in the promotion of granule secretion (Painter & Ginsberg, 1984), while other studies suggest that cytochalasins do not block agonist-mediated granule secretion (Kirkpatrick *et al*, 1980; Cox, 1988). Recent results indicate that the actin cytoskeleton interferes with platelet exocytosis and differentially regulates α-granule and dense granule secretion (Flaumenhaft *et al*, 2005).

We recently demonstrated that the diversity of expression of the Dystrophin associated protein complex (DAPC) plays a key role in the platelet haemostatic functions, participating as a membrane scaffold as well as having a signalling role (Cerecedo *et al*, 2005, 2006a). Dystrobrevins are cytoplasmic components of the DAPC that link the actin cytoskeleton to the extracellular matrix in skeletal muscle (Blake *et al*, 2002); they are the product of two different genes coding for two highly similar proteins, i.e. α- and β-dystrobrevin (Ambrose *et al*, 1997; Peters *et al*, 1997; Blake *et al*, 1998). Dystrobrevins have been characterized in association with dystrophin isoforms and utrophin in several non-muscle tissues including platelets (Cerecedo *et al*, 2005). Functional diversity of α- and β-dystrobrevin within the same cell type has been demonstrated in recent studies in which these proteins bind to the cargo-binding domain of kinesin family member 5A, thus participating in the transport of cellular components (Torreri *et al*, 2005).

The goal of this study was to identify the contribution of actin filaments and microtubules to granule trafficking in adhered platelets. Immunoprecipitation assays and fluorescence resonance energy transfer (FRET) analysis utilizing disrupting cytoskeleton drugs were performed to corroborate that actin filaments and microtubules contribute to α- and dense granule mobilization in adhered platelets, and enabled the identification of the α-dystrobrevins as part of the platelet transport machinery in close association with ubiquitous kinesin heavy chain (UKHC).

Materials and methods

Platelet preparation

Platelets were obtained by venepuncture from healthy donors who had not received any drug during the 10 d prior to sampling and who gave consent for the procedure to be carried out. Blood was immediately mixed with citrate anticoagulant including dextrose at pH 6·5 (93 mmol/l sodium citrate, 70 mmol/l citric acid and 140 mmol/l dextrose) at a blood:anticoagulant ratio of 9:1. Platelet-rich plasma was obtained from total blood by centrifugation at 100 ***g*** for 20 min at room temperature, and was subsequently mixed with an equal volume of citrate anticoagulant and centrifuged at 400 ***g*** for 10 min. (White, 1983). The platelet pack was suspended and washed twice with Hank's balanced saline solution (HBSS) without calcium (137 mmol/l NaCl, 5·3 mmol/l KCl, 1 mmol/l $MgCl_2$, 0·28 mmol/l $Na_2HPO_4.12H_2O$, 0·87 mmol/l NaH_2PO_4, 0·44 mmol/l KH_2PO_4, 4·1 mmol/l $NaHCO_3$, 5·5 mmol/l glucose) and counted in a haematocytometer. Platelets non-specifically activated by the washing were maintained in this solution for 60 min at 37°C in order to achieve a resting condition, which was evaluated by recovery of the discoid shape. All incubations and processing were carried out at room temperature.

Antibodies used

Monoclonal antibodies are referred to as mAb, while polyclonal antibodies are pAb. Actin mAb Cat. no. sc-8432, P-selectin pAb Cat. no. sc-6941, α-dystrobrevin pAb Cat. no. sc-13812, α-tubulin mAb Cat No. sc-5286, β-tubulin pAb Cat no. sc-9110 and UKHC pAb Cat no. sc-28538 were purchased from Santa Cruz Biotechnology, Inc. (Santa Cruz, CA, USA), while serotonin pAb was obtained from Chemicon (Billerica, MA, USA) and β-dystrobrevin was a kind gift of D. Mornet.

Electron microscopy

Spurr resin beds were prepared and polymerized within plastic Petri dishes according to the supplier's instructions (Electron Microscopy Sciences, Fort Washington, PA, USA). Control and 10-μmol/l dimethyl sulphoxide (DMSO) incubated human resting platelets were settled for 1, 5, 10 and 20 min at room temperature on resin beds; each time, non-adhered platelets were washed out with HBSS. Platelets were fixed by incubation with 2·5% glutaraldehyde for 1 h and post-fixed with 1%, OsO_4 in Phosphate-buffered saline (PBS) at 4°C for 30 min. After a thorough washing with PBS, platelets were gradually dehydrated in increasing concentrations of ethanol and then embedded by adding an upper layer of Spurr resin. The resin was polymerized by incubation at 60°C for 24 h (Cerecedo *et al*, 2006b). After the separation of the plastic Petri dish, blocks of the polymerized resin were cut into an ultramicrotome Leica ultracut R (Leica Microsystems, Heidelberg, Germany), and the respective thin sections recovered on copper grids were stained with uranyl acetate and lead citrate, and then examined in a Jeol 2000EX transmission electron microscope (JEOL, Tokyo, Japan) at 80 keV.

Sequence of platelet adhesion to glass and fixation

Platelets (1×10^8/ml) were placed on glass coverslips for 1, 3, 10 and 20 min; non-adherent platelets were removed by

washing with HBSS. Platelets were fixed with 2·5% glutaraldehyde in HBSS for 60 min, and washed and micrographed in a Zeiss Axioskop II phase contrast microscope. For immunofluorescence assays, the same concentration of cells was allowed to adhere to glass slides, and fixed and permeabilized at the same time with a mixture of 2% *p*-formaldehyde, 0·05% glutaraldehyde and 0·04% Nonidet P-40 (NP40) in the cytoskeleton stabilizing solution PHEM [100 mmol/l piperazine diethanesulfonic acid (PIPES), 5·25 mmol/l HEPES, 10 mmol/l ethylene glycol tetraacetic acid (EGTA), 20 mmol/l $MgCl_2$] for 20 min.

Preparation of inhibitors

A 20-μmol/l cytochalasin D (CD) solution (2×) (Sigma Chemical Co., St. Louis, MO, USA) was prepared in HBSS from a 0·507-mmol/l concentrated solution diluted in DMSO. Colchicine (Col; Sigma Chemical Co.) was directly dissolved in HBSS as a 2× solution. 20 μmol/l of paclitaxel (Sigma Chemical Co.) was prepared in PEMG buffer (100 mmol/l PIPES, 10 mmol/l EGTA, 2 mmol/l $MgCl_2$ and 0·1 mmol/l guanosine triphosphate pH 7·0). Finally, jasplakinolide (Molecular Probes, Inc., Eugene, OR, USA) was prepared in HBSS from a 1-mmol/l solution diluted in DMSO.

Treatment of platelets with cytoskeleton inhibitors

Resting platelets (1×10^8/ml) in suspension were incubated with the same volume of the drugs in order to obtain final concentrations of 10 μmol/l of CD, 10 mmol/l Col (Ikeda *et al*, 2000), 8 μmol/l jasplakinolide (Flaumenhaft *et al*, 2005), 30 μmol/l paclitaxel (Patel *et al*, 2005) or a mixture of both inhibitors or stabilizers for 60 min at room temperature.

Evaluation of sP-selectin

Platelets (1×10^8/ml) incubated with cytoskeleton inhibitors were allowed to adhere to glass Petri dishes in a wet camera. After 20 min, the glass Petri dishes with adhered platelets were rinsed with HBSS; supernatants were collected and centrifuged to eliminate non-adhered platelets. Samples were immediately processed for enzyme-linked immunosorbent assay (ELISA) for quantitative detection of soluble human P-selectin levels (sP-selectin; Invitrogen, Camarillo, CA, USA) according to the manufacturer's instructions. Standards were included. Plates were read at 450 nm on a microplate reader (Molecular Devices, Sunnyvale, CA, USA) using SOFT-MAX-PRO software (Molecular Devices). Mean blank reading was subtracted from each sample and control reading. A standard curve was plotted, and the sP-selectin concentration in each sample was determined by interpolation from the standard curve. Three independent experiments were performed, and average standard errors of the mean (±SEM) results are presented graphically.

Immunofluorescence assays

Control platelets and platelets treated with cytoskeleton inhibitors were allowed to adhere to glass coverslips in a wet camera for 20 min; non-adhered cells were removed by washing with HBSS, fixed, and permeabilized with a mixture of 2% *p*-formaldehyde and 0·04% NP40 in PHEM solution (100 mmol/l PIPES, 5·25 mmol/l HEPES, 10 mmol/l EGTA, 20 mmol/l $MgCl_2$). Platelets were first incubated with the specific primary antibodies diluted in PBS 0·1% bovine serum albumin and incubated for 2 h. Cells were washed with PHEM solution and incubated for 1 h with secondary antibody conjugated to Alexa-Fluor-488 or Alexa-Fluor-568 (Molecular Probes) and then washed several times with PHEM and mounted in Vectashield (Vector Laboratories, Inc., Burlingame, CA, USA). Slides were observed using a Leica confocal instrument model TCS-SP5 Mo, lasers were conFigd to 20% (17% outside) for Argon and 45% for He/Ne 543, and images were taken at 63× zoom 6× at 512 × 512 pixels with an HCX PL APO 63×/1·40–0·60 DIL CS oil immersion. Optical sections (*z*) were performed at 118 nm with one Airy unit. Negative controls included cells incubated with an irrelevant polyclonal antibody, and slides were only exposed to secondary antibodies conjugated to the fluorochromes. Likewise, platelets incubated with 0·1% DMSO were processed for 1 h as the solvent control.

Fluorescence resonance energy transfer (FRET) analysis

Fluorescence resonance energy transfer involves the transfer of energy from a fluorescent donor in its excited state to another excitable moiety. FRET requires that the donor molecule's fluorescence emission spectrum overlaps the excitation spectrum of the acceptor molecule. In the present study this overlap corresponded to 50%. FRET analysis was performed confocally in Acceptor Photo Bleaching mode. We used Fluorescein isothiocyanate (FITC)- and Tetramethylrhodamine isothiocyanate (TRITC)-like donor and acceptor-accomplished fluorochromes. The principal line was argon at 20% (33% outside line). Bleaching areas were established by regions of interest and were burned 25 steps. Terminal FRET efficiency for Leica instruments ranged from 0 (0%) to 1 (100%), as established by the multicolor indicative bar.

All immunofluorescence assays to perform FRET analysis were carried out in triplicates from different donors and data are presented as the mean of the efficiency obtained for each experiment. As the standard deviation (SD) of the efficiency values obtained varied from ±0·7 to ±3·7, we decided to report the mean for each value, although the SD values were included in the results section.

Western blotting

Lysates from adhered platelets obtained in sodium dodecyl sulphate (SDS) and β-mercaptoethanol were boiled for 5 min,

subjected to 10% SDS-polyacrylamide gel electrophoresis, and transferred onto nitrocellulose membranes using a semi-dry system (Thermo Electron Co., Milford, MA, USA). Membranes were incubated with appropriate primary antibodies, and then with horseradish peroxidase (HRP)-conjugated secondary antibodies visualized using an enhanced chemoluminescence Western blotting analysis system (Santa Cruz Biotechnology, Inc.), and documented using X-omat film (Kodak, Rochester, NY, USA). Negative controls comprised transferred strips incubated solely with HRP-conjugated secondary antibodies.

Immunoprecipitation assays

Adhered platelets were lysed for 15 min at 4°C with an equal volume of 2× lysis buffer (2 mmol/l EGTA, 100 mmol/l HEPES, 150 mmol/l NaCl, 2% NP40, pH 7·4) containing a protease inhibitor cocktail. Lysates were incubated for 2 h at 4°C with the immunoprecipitating antibodies and subsequently incubated overnight with Rec Protein G-Sepharose (Santa Cruz Biotechnology, Inc.). Immunoprecipitates were separated by centrifugation and washed with NP40-free lysis buffer, then re-suspended in 2× sample buffer (125 mmol/l Tris–HCl, 4% SDS, 20% glycerol, 0·01 mg/ml β-mercaptoethanol and bromophenol blue, pH 6·8) and boiled for 5 min. Immunoprecipitated proteins and supernatants were analyzed by Western blotting.

Statistical analysis

Data obtained from sP-selectin quantification was expressed as mean ± Standard deviation (SD). Statistical analysis was carried out with the Statistical Package for the Social Sciences (SPSS) for Windows version 13 (Microsoft, Chicago, IL, USA). One-way analysis of variance (ANOVA) with a multiple comparison test (Tukey test) was used for data analysis. Statistical significance was defined as $P < 0{\cdot}05$.

Results

Granules are dispersed to the membrane periphery during the adhesion process

We previously described the spatial relationship between the distribution of granules with actin-filament re-organization during the adhesion process by phase contrast microscopy (Cerecedo *et al*, 2002). In order to visualize the sequence of granule dispersion during the adhesion process, we performed electron microscopy analysis of adhered platelets at different intervals of the process. The micrographs taken at 1 min of adhesion showed amplification of the OCS and centralization of the granules at the granulomere zone. A few protrusions, such as filopodia began to be prominent. At 5 min, the filopodia were more abundant, and the plasma membrane began to spread; granules were maintained at the granulomere, however, their presence was observed near the plasma membrane. At 10 and 20 min, lamellipodia were more evident, and the majority of granules were observed close near to the plasma membrane, nearly fusing (arrows). Inserts correspond to phase contrast microscope images of platelets fixed at the times indicated. It is important to note that granules that did not remain in the granulomere were apparently dispersed to the plasma membrane.

To evaluate the influence of cytoskeleton-disrupting agents on granule dispersion, control (DMSO) and treated (with CD and Col) platelets were processed by electron microscopy; platelets adhered to resin beds for 20 min prior to fixation. DMSO exposure did not affect the typical full-spread platelet showing lamellipodium extension, and the granulomere zone was remained apparent. CD inhibited actin-based structure formation during the adhesion process; however, the OCS was slightly enlarged and delocalized, and granules appeared to be fusing with the plasma membrane (Fig 1B, CD arrows). Incipient adhesion structures showed by Col-treated platelets revealed short filopodia, low OSC amplification, and granules surrounding areas of the granulomere zone (Fig 1B, Col). These morphologic studies suggested that upon platelet adhesion, the granules become centralized and classic exocytosis occurs as in nucleated cells via fusion of granules with the plasma membrane.

Actin and tubulin participate in α-granule transport in adhered platelets

It has been established that actin cytoskeleton differentially regulates α-granule and dense granule secretion (Flaumenhaft *et al*, 2005); additionally it has been demonstrated that microtubules play a role in platelet secretion in platelets activated in suspension (Berry *et al*, 1989; Hirata *et al*, 2007). To explore that this assumption was valid in terms of adhered platelets, we performed double immunofluorescence staining using FITC-phalloidin to label actin filaments or microtubules labelled with a secondary FITC antibody, and α-granules containing P-selectin were identified with the aid of an antibody raised against this protein and with a TRITC secondary antibody, in adhered platelets treated with inhibitors of actin filaments and microtubule polymerization (CD and Col, respectively). Additionally, to evaluate the feasible association of α-granules with regard to actin filaments and microtubules, we performed FRET analysis. Actin filaments were distributed from the centre to the cortical zone of the plasma membrane, with bundles radiating to the front of the plasma membrane, while the central zone, associated with the granulomere, was free of label (Fig 2, control). The presence of α-granules was detected at the plasma membrane zone, and these were widely dispersed in the cytoplasm and concentrated at the granulomere zone (Fig 2, control, dotted circle). Merging of the images did not identify a strong association between actin filaments and α-granules, except for scarce zones at the plasma membrane; the FRET value

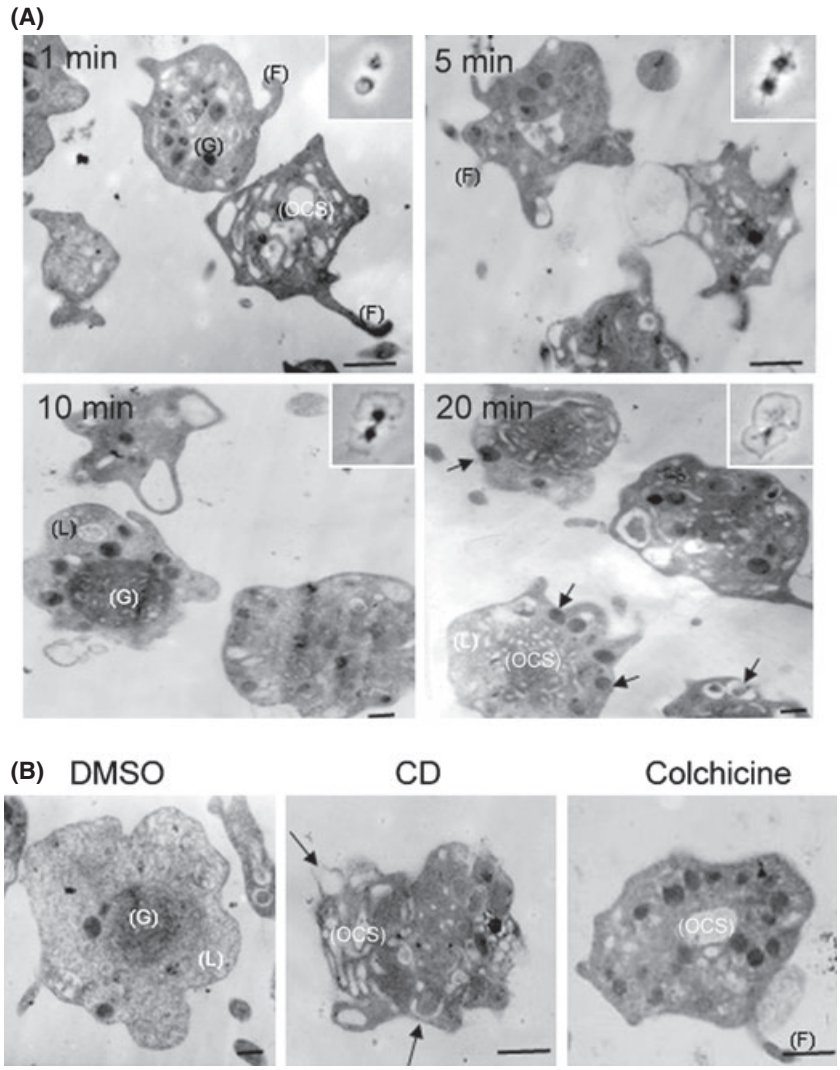

Fig 1. Granule dynamics during the human platelet adhesion process. Panel (A) Electron micrographs of transverse sections of adhered platelets settled for 1, 5, 10 and 20 min and processed by transmission electron microscopy. Granules are centralized at the granulomere (G), but as the platelet adhesion process continues, the granules are translocated to the plasma membrane, fusing with it (arrows). (F) filopodia, (L) lamellipodia, OCS (open canalicular system). Micrographs are representative of triplicates. Scale bar: 1 μm. Panel (B) Electron micrographs of transverse sections of adhered platelets treated with the vehicle (DMSO), 10 μmol/l cytochalasin D (CD) and 10 mmol/l colchicine (Col) and settled for 20 min. Platelets were then processed by transmission electron microscopy. (F) filopodia, (G) granulomere, (L) lamellipodia, OCS (open canalicular system). Micrographs are representative of triplicates. Scale bar: 1 μm.

corresponded to 90% ± 2·08, observed as red discrete zones at the plasma membrane (Fig 2, control arrowheads).

Full-adhered platelets showed fragmentation of the original microtubule ring and re-distribution of tubulin through the cytoplasm or beneath the plasma membrane. α-Granules and microtubules appeared to co-localize at the granulomere zone (Fig 2, control dotted circle) and at the periphery of the plasma membrane, represented by red dots with the FRET analysis and with an efficiency value corresponding to 90% ± 3·7 (Fig 2, control arrowheads), similar to that observed between actin filaments and α-granules.

Treatment with CD prevented actin bundling, and although actin filaments were observed at the plasma membrane, cytoplasmic aggregates of actin were evident at the site of the contractile ring (Fig 2, CD). α-Granules maintained a cytoplasmic concentrated homogeneous distribution. The FRET value obtained under these conditions (73% ± 2·12) revealed a diminution in the feasible association of α-granules and actin filaments, but co-localization remained at the plasma membrane (Fig 2, CD, arrowheads), while diminution of the association between α-granules and microtubules under these same conditions was not lower (85% ± 0·7) and red spots were observed with FRET images at the plasma membrane (Fig 2, CD, arrowheads).

Platelets treated with Col, an inhibitor of microtubule polymerization, were not observed as fully extended and did

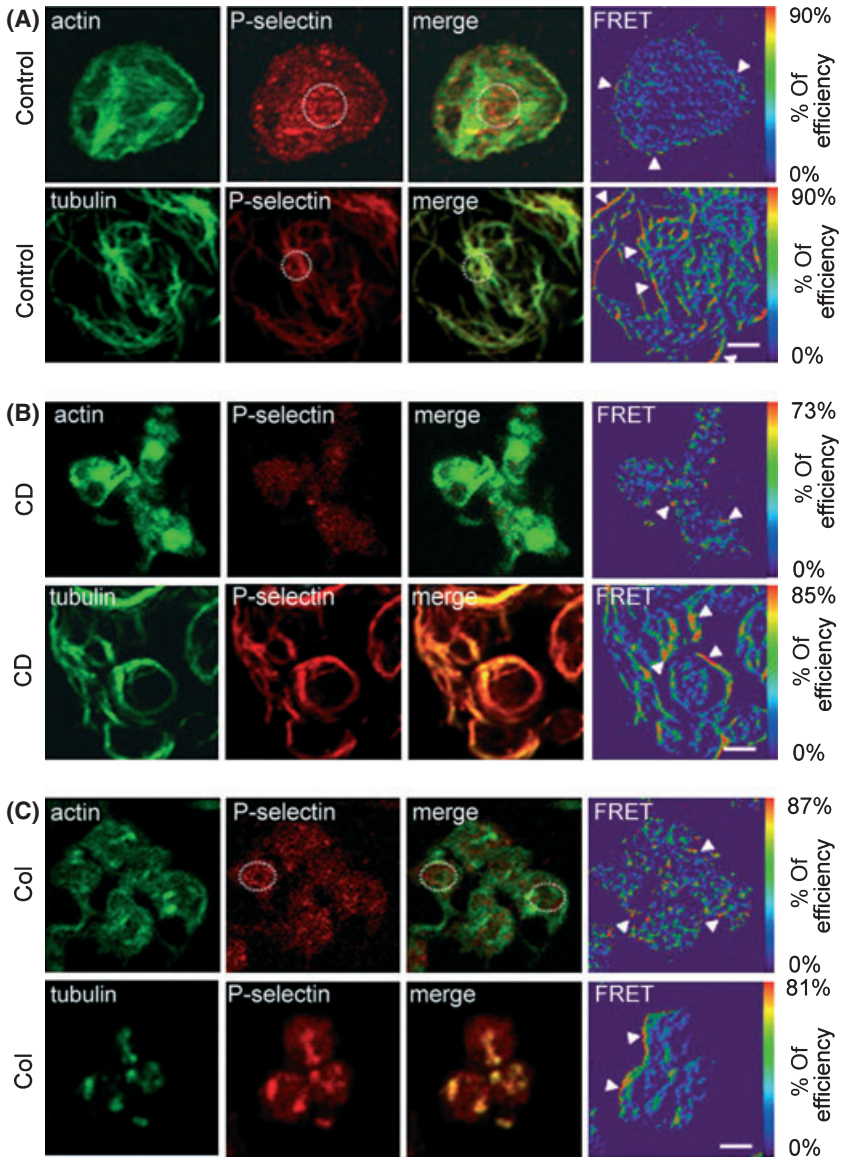

Fig 2. Actin cytoskeleton and microtubules participate in α-granule dispersion in adhered platelets. Panel (A) Resting platelets were adhered on glass for 20 min and analyzed by confocal microscopy after processing for double-labelling, using fluorescein isothiocyanate (FITC)-phalloidin to detect actin filaments and α-tubulin antibody, followed by a secondary FITC antibody, and P-selectin antibody identified with a tetramethyl rhodamine isocyanate (TRITC) secondary antibody. The respective merged images, as well as the means of fluorescence resonance energy transfer (FRET) analysis, are shown. Granulomere zone (dotted circle), co-localization areas (arrowheads). Scale bar = 2 μm. Panel (B) Resting platelets were incubated with cytochalasin D (CD) for 60 min, adhered on glass, and analyzed by confocal microscopy after processing for double-labelling, using FITC-phalloidin to detect actin filaments and α-tubulin antibody, followed by a FITC secondary antibody and P-selectin, identified with a TRITC antibody. The respective merged images, as well as the means of FRET analysis, are shown. Co-localization areas (arrowheads). Scale bar = 2 μm. Panel (C) Resting platelets were incubated with Col for 60 min, adhered on glass, and analyzed by confocal microscopy after processing for double-labelling, using FITC-phalloidin to detect actin filaments and α-tubulin antibody, followed by a FITC secondary antibody and P-selectin identified with a TRITC antibody. The respective merged images, as well as the means of FRET analysis, are shown. Granulomere zone (dotted circle), co-localization areas (arrowheads). Scale bar = 2 μm.

not display typical actin-based structures; however, the contractile rings were conserved (Fig 2, Col, dotted circles). α-Granules and actin filaments remained associated at the plasma membrane and were clearly observed in the FRET images (Fig 2, Col, arrowheads), whose value corresponded to 87% ± 0·7; this value was similar to that exhibited by control platelets. In contrast, α-granules and microtubules reduced their feasible association, demonstrating a FRET value of 81% ± 1·0 with evident red extended zones at the periphery (Fig 2, Col, arrowheads). These results showed that microfilaments and microtubules could be associated with α-granules because depolymerization of both systems reduced their association.

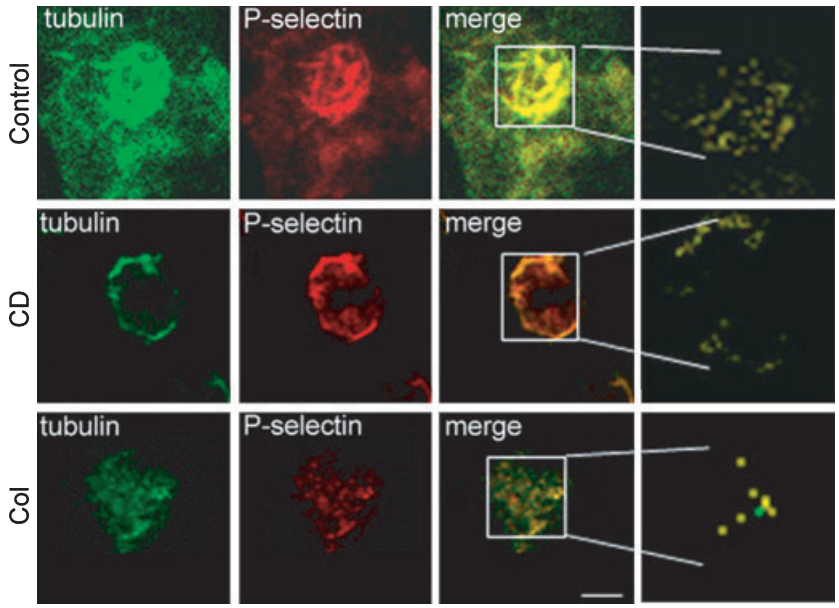

Fig 3. Microtubules modulate α-granule trafficking to the plasma membrane. Resting platelets were incubated with cytochalasin D (CD) and colchicine (Col) for 60 min, adhered on glass, and analyzed by confocal microscopy to obtain optical sections (*z*) at 0·8 μm. Double immunolocalization was performed using α-tubulin antibody revealed with a fluoroscein isothiocyanate (FITC) secondary antibody and P-selectin to stain α-granules evidenced with a tetramethyl rhodamine isocyanate (TRITC) secondary antibody. The boxed areaa are also shown as enlarged images. Scale bar = 2 μm.

Microtubules interact with α-granules at the granulomere zone

In order to confirm the feasible co-localization of α-granules and microtubules at granulomere zones, double immunofluorescence labelling was performed in fully adhered control platelets and in platelets treated with inhibitors of actin and microtubule polymerization. Microtubules were observed using a primary antibody directed against α-tubulin and a secondary antibody labelled with FITC; α-granules were identified using the primary antibody raised against P-selectin and were revealed with a TRITC secondary antibody. Optical sections evaluated at 0·8 μm showed that the main co-localization between microtubules and α-granules was localized at the granulomere zone of full-spread platelets, as amplification was demonstrated (Fig 3, Control). Platelets adhered in presence of CD showed α-granule distribution confined to the microtubule position at the plasma membrane (Fig 3, CD). Microtubule disturbance employing Col generated images in which α-granules were co-distributed with depolymerizing tubulin fragments at the cytoplasm and at the boundaries of the plasma membrane (Fig 3, Col).

Actin and tubulin participate in dense-granule diffusion in adhered platelets

To observe whether there was any difference in the association pattern between dense granules compared with those observed

Fig 4. Actin cytoskeleton and microtubules participate in dense granule dispersion in adhered platelets. Panel (A) Resting platelets were adhered on glass for 20 min and analyzed by confocal microscopy after processing for double-labelling, using fluorescein isothiocyanate (FITC)-phalloidin to detect actin filaments and α-tubulin antibody, followed by a secondary FITC antibody and serotonin antibody, identified with a tetramethyl rhodamine isocyanate (TRITC) secondary antibody. The respective merged images, as well as the means of fluorescence resonance energy transfer (FRET) analysis, are shown. Granulomere zone (dotted circle), co-localization areas (arrowheads). Scale bar = 2 μm. Panel (B) Resting platelets were incubated with cytochalasin D (Cit D) for 60 min, adhered on glass, and analyzed by confocal microscopy after processing for double-labelling, using FITC-phalloidin to detect actin filaments and α-tubulin antibody, followed by a FITC secondary antibody and serotonin, identified with a TRITC antibody. The respective merged images, as well as the means of FRET analysis, are shown. Co-localization areas (arrowheads). Scale bar = 2 μm. Panel (C) Resting platelets were incubated with Col for 60 min, adhered on glass, and analyzed by confocal microscopy after processing for double-labelling, using FITC-phalloidin to detect actin filaments and α-tubulin antibody, followed by a FITC secondary antibody and serotonin evidenced with a TRITC antibody. The respective merged images, as well as the means of FRET analysis, are shown. Granulomere zone (dotted circle), co-localization areas (arrowheads). Scale bar = 2 μm. Panel (D) Resting platelets were adhered on glass and processed for immunoprecipitation assays using anti-actin, anti-a-tubulin and anti-P-selectin antibodies (IP). Proteins from total extracts (E) and immunoprecipitates (Ip) were analyzed by immunoblot utilizing antibodies against actin, tubulin, serotonin and P-selectin. Actin and tubulin were detected with bands of 42- and 55 kDa, respectively, while the granule contents of serotonin and P-selectin showed bands of 175- and 140 kDa, respectively.

with α-granules and actin filaments or microtubules, double immunofluorescence and FRET analysis was performed in fully adhered platelets (Fig 4A) and in platelets treated with CD and Col (Fig 4B, C, respectively). FITC-phalloidin was used to label actin filaments or microtubules labelled with an anti-tubulin, and a secondary FITC antibody was utilized. Serotonin as a component of dense granules was labelled with a respective antibody and with a TRITC secondary antibody. Upon activation to glass, serotonin was mainly redistributed to the granulomere, but was also observed at the cytoplasm and

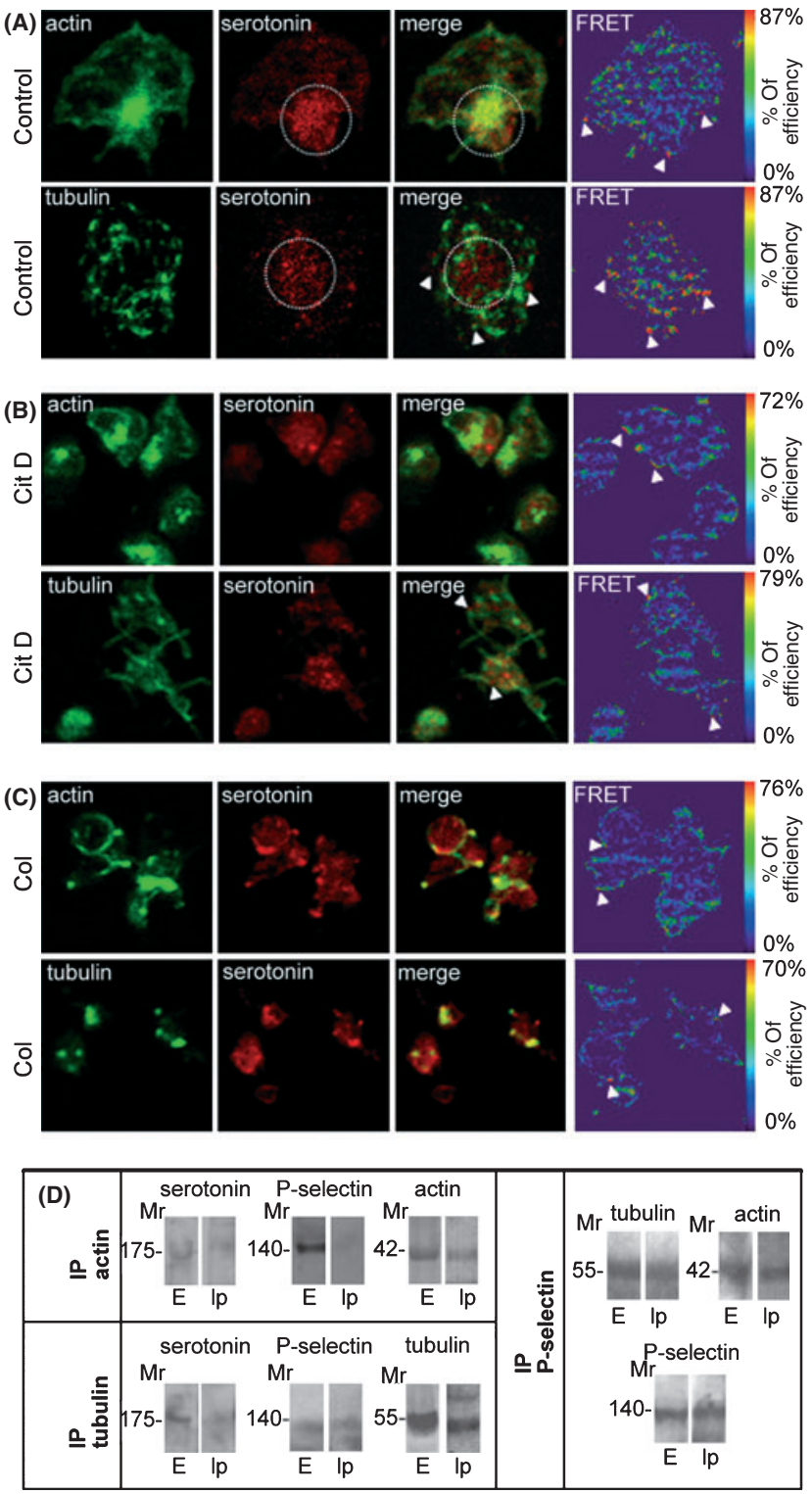

plasma membrane, co-localizing with actin at these zones (Fig 4, control dotted circle). Co-distribution of serotonin with microtubules was also observed as concentrated at the granulomere (dotted circle) and scarcely at the plasma membrane. The association of dense granules with actin filaments and microtubules was better observed with FRET images, in which red dots were very evident, especially at the plasma membrane (Fig 4, control arrows). FRET values showed a feasible association between dense granules and actin filaments or microtubules (87% ± 1·15 and ± 2·64 respectively) that was very similar to that observed with α-granules (Fig 3A). It is noteworthy that dense granules co-localized preferentially with actin filaments at the cell periphery; in contrast, dense granules and microtubules were co-distributed throughout the cytoplasm and at the plasma membrane (Fig 4, Control arrowheads).

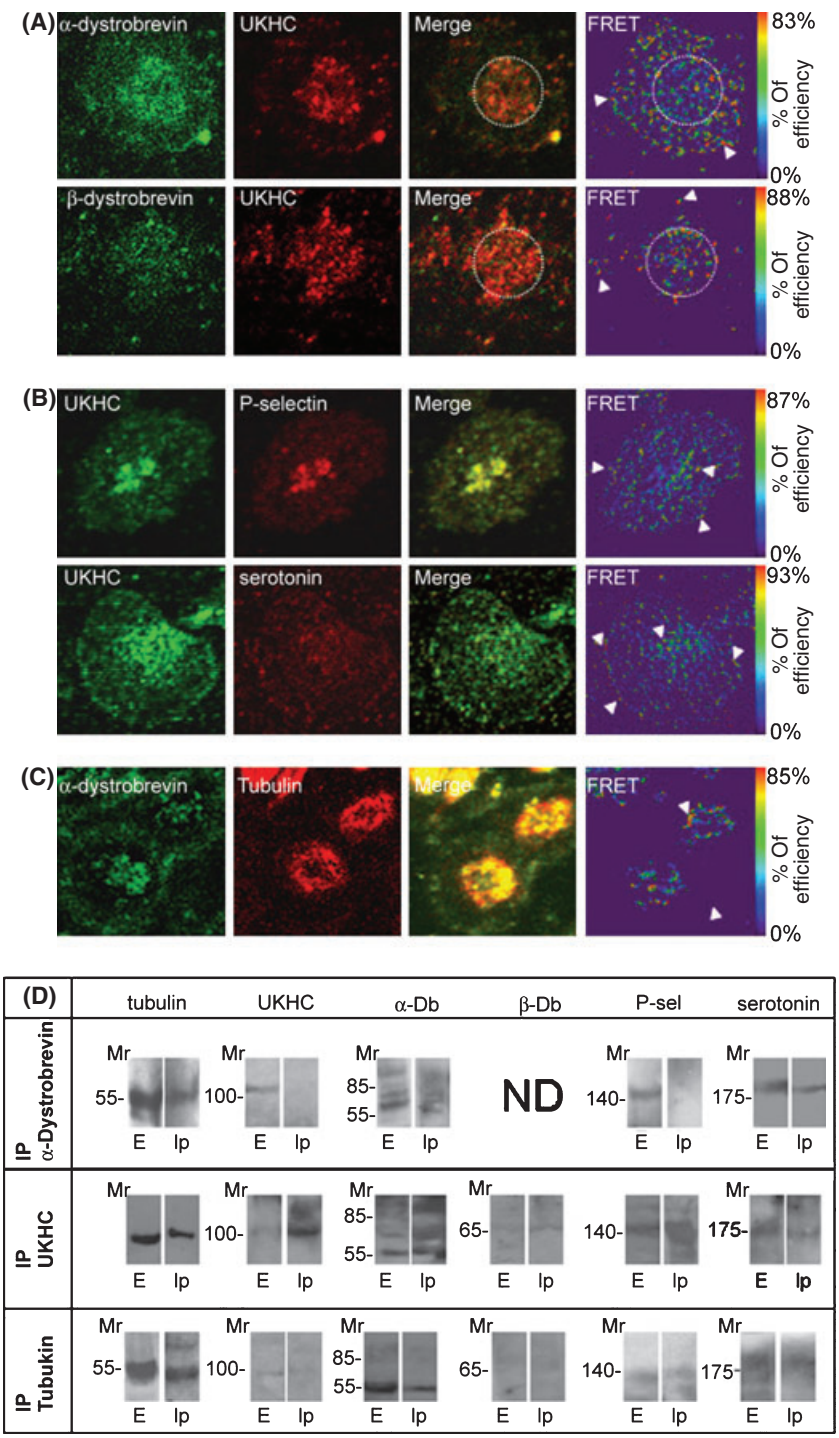

© 2010 Blackwell Publishing Ltd,

The presence of CD reduced the association of dense granules with actin filaments (72% ± 3·6), as well as that with microtubules (79% ± 3·3) in relation to the controls (Fig 3B). However, use of Col induced a lower FRET value (70% ± 3·7), inhibiting microtubule polymerization as well as the association with dense granules revealed with red discrete dots (arrowheads). Col also affected the association of actin filaments and dense granules, giving a low FRET value (76% ± 2·12); however, unlike that observed with actin filaments, tubulin co-localized with dense granules not only at the plasma membrane, but also at the cytoplasm (arrowheads).

To corroborate the data obtained by confocal and FRET analysis, we performed immunoprecipitation assays from fully adhered platelet extracts using actin, tubulin and P-selectin antibodies. Total extracts and protein- Immunoprecipitated (Ip) extracts were resolved by Western blot (Fig 4D).

The results of the pull-down assay utilizing anti-actin antibody showed that actin was precipitated only with serotonin and not with P-selectin (Fig 4D, Ip actin). In contrast, immunoprecipitates obtained with tubulin antibody contained serotonin and P-selectin. Complementary immunoprecipitation assays performed with P-selectin antibody pulled down actin and tubulin (Fig 4D, Ip P-selectin). Together, these results show that actin filaments and microtubules participate in granule distribution in adhered platelets. Although there was a depolymerizing treatment of actin filaments or microtubules, the system is organized to ensure that granule distribution is obtained.

Motor protein and α-dystrobrevins are implicated in granule trafficking of adhered platelets

Kinesin was previously identified as a novel dystrobrevin-interacting protein (Macioce *et al*, 2003), and we have described the presence of α-dystrobrevin-1 and -2, as well as β-dystrobrevin in platelets (Cerecedo *et al*, 2005). This led us to consider the possibility that a function of dystrobrevins tethered to microtubules exists to provide a track for kinesin to reach the plasma membrane.

This possibility was tested by processing double immunofluorescence labelling and FRET analysis of adhered platelets, using α-dystrobrevins and β-dystrobrevin antibodies labelled with a FITC secondary antibody and a UKHC revealed with a TRITC secondary antibody. Extensive areas of co-localization between α- and β-dystrobrevins and UKHC were mainly located at the granulomere zone (Fig 5, dotted circles). Efficiency found by FRET analysis suggested that the UKHC was associated with α-dystrobrevins (83% ± 1·5) more importantly at the cytoplasm and the plasma membrane (arrowheads), while the association with β-dystrobrevin (88% ± 1·73) was mainly at the granulomere zone.

Feasible association between UKHC and both types of platelet granules was performed using the UKHC antibody and P-selectin or serotonin as components of α- and of dense granules, respectively. Both granule types were similarly re-distributed in the granulomere, cytoplasm and plasma membrane (arrowheads at FRET images). FRET values confirmed the feasible association with values of 87% ± 3·5 and 93% ± 3·4 for α- and dense granules with UKHC, respectively.

α-Dystrobrevins that preferentially co-distributed with microtubules were more evident as patches at the granulomere zone and at the plasma membrane, with co-localization revealed by red points in this region, as well as in the cell periphery in FRET images, whose value corresponded to 85% ± 2·7 (Fig 4C, arrowheads). To confirm our immunofluorescence and FRET analysis results, adhered platelet extracts were processed for immunoprecipitation assays using antibodies directed against α-dystrobrevins, UKHC and tubulin. Total extracts as well as immunoprecipitates were revealed by Western blot for tubulin, UKHC, α-dystrobrevin, β-dystrobrevin, P-selectin and serotonin. α-dystrobrevins immunoprecipitated tubulin and serotonin, but not UKHC and P-selectin. In contrast, UKHC pulled down tubulin, α-dystrobrevins, β-dystrobrevins and components of α- or dense granules (P-selectin and serotonin), while tubulin-obtained immunoprecipitates showed clear bands that showed the presence of P-selectin, serotonin and α-dystrobrevins, in addition to faint bands corresponding to UKHC and β-dystrobrevins.

Fig 5. α-Dystrobrevins participate in platelet adhered granules. Panel (A) Resting platelets were adhered on glass for 20 min and analyzed by confocal microscopy after processing for double-labelling, using α- and β-dystrobrevin antibodies revealed with fluorescein isothiocyanate (FITC) and ubiquitous kinase heavy chain (UKHC) antibody, identified with a tetramethyl rhodamine isocyanate (TRITC) secondary antibody. The respective merged images, as well as the means of Fluorescence resonance energy transfer (FRET) analysis, are shown. Granulomere zone (dotted circle), co-localization areas (arrowheads). Scale bar = 2 μm. Panel (B) Resting platelets were adhered on glass for 20 min and analyzed by confocal microscopy after processing for double-labelling. Using a UKHC antibody revealed with FITC and P-selectin and serotonin antibodies, identified with a TRITC secondary antibody. The respective merged images, as well as the means of FRET analysis, are shown. Co-localization areas (arrowheads). Scale bar = 2 μm. Panel (C) Resting platelets were adhered on glass for 20 min and analyzed by confocal microscopy after processing for double-labelling, using α-dystrobrevin antibody revealed with FITC and α-tubulin antibody, identified with a TRITC secondary antibody. The respective merged images, as well as the means of the FRET analysis, are shown. Granulomere zone (dotted circle), co-localization areas (arrowheads). Scale bar = 2 μm. Panel (D) Resting platelets were adhered on glass and processed for immunoprecipitation assays using anti-UKHC, anti-α-dystrobrevin and anti-α-tubulin antibodies (IP). Proteins from total extracts (E) and Immunoprecipitates (Ip) were analyzed by immunoblot utilizing antibodies against tubulin, UKHC, α-dystrobrevin, β-dystrobrevin, P-selectin and serotonin. Tubulin and UKHC were detected with bands of 55- and 100 kDa; α-dystrobrevin-1 and -2 were identified by bands of 55- and 85 kDa, respectively. β-dystrobrevin was observed by a band of 65 kDa while the granule contents of serotonin and P-selectin showed bands of 175- and 140 kDa, respectively. ND, not done.

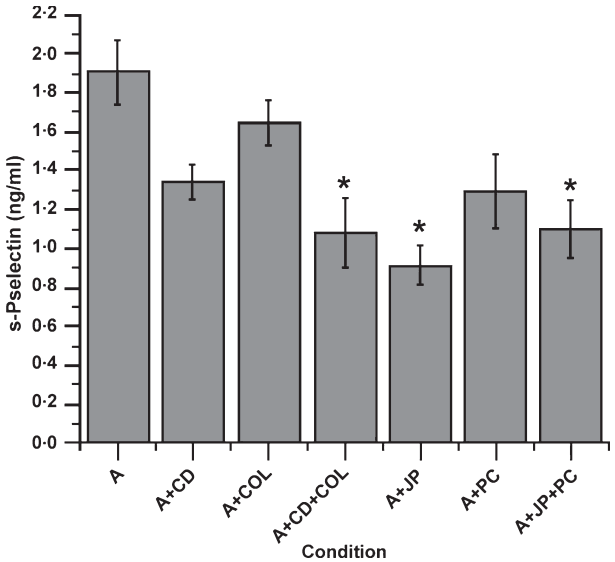

Fig 6. Actin and microtubules are involved in granule dispersion. Control adhered platelets (A) and adhered platelets treated with cytochalasin D (A+CD), colchicine (A+Col), both inhibitors simultaneously (A+CD+Col), jasplakinolide (A+JP), paclitaxel (A+PC), and both stabilizers simultaneously (A+JP+PC) were adhered on glass for 20 min. Supernatants were isolated and quantified for sP-selectin by enzyme-linked immunosorbent assay (ELISA) (*$P < 0{\cdot}05$) n = three independent experiments. Error bars represent standard error of the mean (±SEM).

Granule dispersion depends on actin filaments and microtubules

To explore the biological participation of actin filaments and microtubules in α- granule dispersion, $1{\cdot}5 \times 10^6$ platelets/μl were incubated in the presence of the depolymerizing drugs, CD and Col and a mixture of both, as well as with stabilizing the cytoskeleton drugs jasplakinolide (for actin filaments), paclitaxel (for microtubules) and a mixture of both before they were adhered. Soluble P-selectin, obtained from supernatants of adhered platelets, was quantified using an ELISA (Fig 6).

Control supernatant obtained from platelets without drugs had a mean sP-selectin concentration of 1·90 ng/ml, while supernatants of platelets treated with CD or Col showed a reduced sP-selectin concentration relative to control supernatants, with mean values of 1·33 and 1·64 ng/ml, respectively. In contrast, the mean value for platelet supernatants treated with both inhibitors corresponded to 1·49 ng/ml. Supernatants from platelets treated with jasplakinolide and paclitaxel showed mean values similar to those observed in the presence of poisons, but lower values compared with controls corresponding to 0·915 ng/ml for jasplakinolide and 1·291 ng/ml for paclitaxel. Simultaneous treatment with both stabilizers rendered a value of 1·1 ng/ml. One-way ANOVA analysis and Tukey multiple comparisons showed that sP-selectin levels in supernatants employing jasplakinolide as well as simultaneous two depolymerizing or two stabilizer drugs were statistically significant ($P < 0{\cdot}05$; Fig 6). These results strongly suggested that microtubules as well as actin filaments actively participated in α-granule trafficking of adhered platelets.

Discussion

Dramatic platelet shape change upon surface activation involves the fragmentation of the microtubule ring, as well as the formation of actin-based structures, such as the contractile ring (Bearer, 1995), which provokes concurrent centralization of granules preceding granule-content release. However, the influence of the cytoskeleton on granule secretion has been a controversial subject. Inhibition of tubulin using monoclonal antibodies inhibited platelet granule secretion; in contrast, the microtubule stabilizing agent paclitaxel suggested that microtubule reorganization does not influence granule secretion (White & Rao, 1982, 1983). F-actin disassembly might be required for normal granule secretion, because studies utilizing actin polymerization inhibitors did not block agonist-mediated granule secretion (Kirkpatrick *et al*, 1980; Cox, 1988; Lefebvre *et al*, 1993). Additionally, it has been demonstrated that the actin cytoskeleton interferes with platelet exocytosis and differentially regulates α-granule and dense granule secretion (Flaumenhaft *et al*, 2005). However, it is important to note that similar studies have not been described in adhered platelets.

Our morphological analysis confirmed that initially, platelet granules were centralized to the granulomere; however, as the process continued, they were translocated near the plasma membrane. We also observed that granule dispersion can proceed in the absence of microtubules or microfilaments, although with different distribution patterns.

Recently, using the microtubule-inhibitor Col and the actin filament-inhibitor CD, we found that microtubules and actin filaments were highly dependent upon each other, and that removing either component dramatically changed the organization of the other (Cerecedo *et al*, 2008). It is evident that platelet cell spreading requires extensive cellular remodelling, which was inhibited by treatment with CD or Col, as well as with jasplakinolide or taxol. The present study showed that the reduced sP-selectin levels observed following independent treatment with depolymerizing or stabilizing drugs was not statistically significant, except for jasplakinolide, as well as for simultaneous treatment with both cytoskeleton inhibitors and both cytoskeleton stabilizers. In all cases, granule-content extrusion was diminished, but not prevented, as reflected in sP-selectin levels.

In addition, it is very probable that the low quantities of sP-selectin observed with simultaneous use of stabilizer or inhibitor drugs was due to the feasible fusion of the membrane granule with the membranous system, which is a critical event for the release of platelet granule contents into the extracellular environment (Furie *et al*, 2001; Zhou & Freed, 2009). It is probable that the interaction between granules and cytoplasm membranes or OCS was too close, thus, it was not affected by

the use of cytoskeleton inhibitors or stabilizers. It is also feasible that jasplakinolide interrupted granule centralization and that amplification of the OCS in a greater extension disturbed the re-distribution of microtubules, thus the occurrence of granule translocation to the plasma membrane.

According to our results, it is pertinent to propose that microtubules, probably via kinesin motors, counteract the confining effect of the actin-based contractile ring by increasing short-range mobility of granules at the plasma membrane. Thus, actin and microtubules may play opposing and complementary roles in order to fine-tune mobility and to direct granules at target sites on the plasma membrane. At these sites, the fusing membranes are orchestrated by the universal machinery denominated Soluble *N*-ethylmaleimide (NEM)-sensitive attachment protein receptors (SNARE) (Lemons *et al*, 1997; Flaumenhaft *et al*, 1999).

In neurons, motor proteins, such as kinesin, transport cargoes along microtubules and are involved in the targeting and localization of specific proteins within distinct molecular and functional domains. Recent studies have suggested a role for dystrobrevin as a motor protein receptor binding to the cargo-binding domain of the kinesin heavy chain (Ceccarini *et al*, 2005).

The present study found that co-distribution of α-dystrobrevins with kinesin and microtubules in the granulomere zone strongly suggest that α-dystrobrevins might play a role in granule transport as an adaptor molecule upon surface adhesion.

In conclusion, we speculate that granule dynamics during the adhesion process is strictly regulated by actin filaments and microtubules. This begins with the centralization of granules at the granulomere zone by the actin-based contractile ring; however, as the process continues, microtubules are re-organized from the granulomere, translocating the granules to the plasma membrane by kinesin motors. During this process, α-dystrobrevins play a modulator active role in mediating the recruitment of motor proteins to granules.

References

Ambrose, H.J., Blake, D.J., Nawrotzki, R.A. & Davies, K.E. (1997) Genomic organization of the mouse dystrobrevin gene: comparative analysis with the dystrophin gene. *Genomics*, **39,** 359–369.

Anitua, E., Andia, I., Ardanza, B., Nurden, P. & Nurden, A.T. (2004) Autologous platelets as a source of proteins for healing and tissue regeneration. *Thrombosis and Haemostasis*, **91,** 4–15.

Bearer, E.L. (1995) Cytoskeletal domains in the activated platelet. *Cell Motility and the Cytoskeleton*, **30,** 50–66.

Berry, S., Dawicki, D.D., Agarwal, K.C. & Steiner, M. (1989) The role of microtubules in platelet secretory release. *Biochimica et Biophysica Acta*, **1012,** 46–56.

Blake, D.J., Nawrotzki, R., Loh, N.Y., Gorecki, D.C. & Davies, K.E. (1998) beta-dystrobrevin, a member of the dystrophin-related protein family. *Proceedings of the National Academy of Sciences of the United States of America*, **95,** 241–246.

Blake, D.J., Weir, A., Newey, S.E. & Davies, K.E. (2002) Function and genetics of dystrophin and dystrophin-related proteins in muscle. *Physiological Reviews*, **82,** 291–329.

Ceccarini, M., Torreri, P., Lombardi, D.G., Macchia, G., Macioce, P. & Petrucci, T.C. (2005) Molecular basis of dystrobrevin interaction with kinesin heavy chain: structural determinants of their binding. *Journal of Molecular Biology*, **354,** 872–882.

Cerecedo, D., Stock, R., Gonzalez, S., Reyes, E. & Mondragon, R. (2002) Modification of actin, myosin and tubulin distribution during cytoplasmic granule movements associated with platelet adhesion. *Haematologica*, **87,** 1165–1176.

Cerecedo, D., Martinez-Rojas, D., Chavez, O., Martinez-Perez, F., Garcia-Sierra, F., Rendon, A., Mornet, D. & Mondragon, R. (2005) Platelet adhesion: structural and functional diversity of short dystrophin and utrophins in the formation of dystrophin-associated-protein complexes related to actin dynamics. *Thrombosis and Haemostasis*, **94,** 1203–1212.

Cerecedo, D., Mondragon, R., Cisneros, B., Martinez-Perez, F., Martinez-Rojas, D. & Rendon, A. (2006a) Role of dystrophins and utrophins in platelet adhesion process. *British Journal of Haematology*, **134,** 83–91.

Cerecedo, D., Gonzalez, S., Mondragon, M., Reyes, E. & Mondragon, R. (2006b) In-vitro model for the ultrastructural study of the formation of thrombi in human platelets. *Blood Coagulation and Fibrinolysis*, **17,** 161–164.

Cerecedo, D., Cisneros, B., Suarez-Sanchez, R., Hernandez-Gonzalez, E. & Galvan, I. (2008) beta-Dystroglycan modulates the interplay between actin and microtubules in human-adhered platelets. *British Journal of Haematology*, **141,** 517–528.

Coppinger, J.A., Cagney, G., Toomey, S., Kislinger, T., Belton, O., McRedmond, J.P., Cahill, D.J., Emili, A., Fitzgerald, D.J. & Maguire, P.B. (2004) Characterization of the proteins released from activated platelets leads to localization of novel platelet proteins in human atherosclerotic lesions. *Blood*, **103,** 2096–2104.

Cox, A.C. (1988) Cytochalasin E enhances the protein kinase C-dependent process of secretion. *Biochemical and Biophysical Research Communications*, **150,** 745–751.

Escolar, G. & White, J.G. (1991) The platelet open canalicular system: a final common pathway. *Blood Cells*, **17,** 467–485.

Escolar, G., Leistikow, E. & White, J.G. (1989) The fate of the open canalicular system in surface and suspension-activated platelets. *Blood*, **74,** 1983–1988.

Flaumenhaft, R., Croce, K., Chen, E., Furie, B. & Furie, B.C. (1999) Proteins of the exocytotic core complex mediate platelet alpha-granule secretion. Roles of vesicle-associated membrane protein, SNAP-23, and syntaxin 4. *Journal of Biological Chemistry*, **274,** 2492–2501.

Flaumenhaft, R., Dilks, J.R., Rozenvayn, N., Monahan-Earley, R.A., Feng, D. & Dvorak, A.M. (2005) The actin cytoskeleton differentially regulates platelet alpha-granule and dense-granule secretion. *Blood*, **105,** 3879–3887.

Furie, B., Furie, B.C. & Flaumenhaft, R. (2001) A journey with platelet P-selectin: the molecular basis of granule secretion, signalling and cell adhesion. *Thrombosis and Haemostasis*, **86,** 214–221.

Ginsberg, M.H., Taylor, L. & Painter, R.G. (1980) The mechanism of thrombin-induced platelet factor 4 secretion. *Blood*, **55,** 661–668.

Hirata, Y., Broquet, A.H., Menchen, L. & Kagnoff, M.F. (2007) Activation of innate immune defense mechanisms by signaling through

RIG-I/IPS-1 in intestinal epithelial cells. *Journal of Immunology*, **179,** 5425–5432.

Ikeda, Y., Martone, M., Gu, Y., Hoshijima, M., Thor, A., Oh, S.S., Peterson, K.L. & Ross, Jr, J. (2000) Altered membrane proteins and permeability correlate with cardiac dysfunction in cardiomyopathic hamsters. *American Journal of Physiology. Heart and Circulatory Physiology*, **278,** H1362–H1370.

Kirkpatrick, J.P., McIntire, L.V., Moake, J.L. & Cimo, P.L. (1980) Differential effects of cytochalasin B on platelet release, aggregation and contractility: evidence against a contractile mechanism for the release of platelet granular contents. *Thrombosis and Haemostasis*, **42,** 1483–1489.

Lefebvre, P., White, J.G., Krumwiede, M.D. & Cohen, I. (1993) Role of actin in platelet function. *European Journal of Cell Biology*, **62,** 194–204.

Lemons, P.P., Chen, D., Bernstein, A.M., Bennett, M.K. & Whiteheart, S.W. (1997) Regulated secretion in platelets: identification of elements of the platelet exocytosis machinery. *Blood*, **90,** 1490–1500.

Macioce, P., Gambara, G., Bernassola, M., Gaddini, L., Torreri, P., Macchia, G., Ramoni, C., Ceccarini, M. & Petrucci, T.C. (2003) Beta-dystrobrevin interacts directly with kinesin heavy chain in brain. *Journal of Cell Science*, **116,** 4847–4856.

Painter, R.G. & Ginsberg, M.H. (1984) Centripetal myosin redistribution in thrombin-stimulated platelets. Relationship to platelet Factor 4 secretion. *Experimental Cell Research*, **155,** 198–212.

Patel, S.R., Richardson, J.L., Schulze, H., Kahle, E., Galjart, N., Drabek, K., Shivdasani, R.A., Hartwig, J.H. & Italiano, Jr, J.E. (2005) Differential roles of microtubule assembly and sliding in proplatelet formation by megakaryocytes. *Blood*, **106,** 4076–4085.

Peters, M.F., O'Brien, K.F., Sadoulet-Puccio, H.M., Kunkel, L.M., Adams, M.E. & Froehner, S.C. (1997) beta-dystrobrevin, a new member of the dystrophin family. Identification, cloning, and protein associations. *Journal of Biological Chemistry*, **272,** 31561–31569.

Rendu, F. & Brohard-Bohn, B. (2001) The platelet release reaction: granules' constituents, secretion and functions. *Platelets*, **12,** 261–273.

Sneddon, J.M. (1971) Effect of mitosis inhibitors on blood platelet microtubules and aggregation. *Journal of Physiology*, **214,** 145–158.

Stenberg, P.E., Shuman, M.A., Levine, S.P. & Bainton, D.F. (1984) Redistribution of alpha-granules and their contents in thrombin-stimulated platelets. *Journal of Cell Biology*, **98,** 748–760.

Torreri, P., Ceccarini, M., Macioce, P. & Petrucci, T.C. (2005) Biomolecular interactions by Surface Plasmon Resonance technology. *Annali dell Istituto Superiore di Sanita*, **41,** 437–441.

White, J.G. (1983) Ultrastructural physiology of platelets with randomly dispersed rather than circumferential band microtubules. *American Journal of Pathology*, **110,** 55–63.

White, J.G. & Escolar, G. (1991) The blood platelet open canalicular system: a two-way street. *European Journal of Cell Biology*, **56,** 233–242.

White, J.G. & Rao, G.H. (1982) Effects of a microtubule stabilizing agent on the response of platelets to vincristine. *Blood*, **60,** 474–483.

White, J.G. & Rao, G.H. (1983) Influence of a microtubule stabilizing agent on platelet structural physiology. *American Journal of Pathology*, **112,** 207–217.

Zhou, W. & Freed, C.R. (2009) Adenoviral gene delivery can reprogram human fibroblasts to induced pluripotent stem cells. *Stem Cells*, **27,** 2667–2674.